VOLTAGE SENSORLESS BASED VIRTUAL FLUX CONTROL OF THREE LEVEL NPC BACK-TO-BACK CONVERTER DFIGUNDER GRID FAULT

Imad Merzouk[1], Mohamed Mounir Rezaoui[1], Noureddine Bessous[2*], Abdsalem Gafazi[1]

[1]*LAADI, Faculty of Science and Technology, University of Djelfa 17000 DZ, ALGERIA*
[2]*Faculty of Science and Technology, University of El Oued 39000 DZ, ALGERIA*

Email*: nbessous@yahoo.fr

Abstract – *In this paper, a harmonic elimination of grid and stator currents of doubly fed induction generator (DFIG) in case of grid fault without line voltage sensors is proposed . This can be achieved by compensating power based on virtual flux voltage sensorless technique. Direct power control with space vector modulation (DPC-SVM) is used to control both grid-side (GSC)and rotor-side converters (RSC). To achieve the control objective, compensated active and reactive powers are calculated based on virtual flux technique with balanced and harmonic free current as a control target. A theoretical analysis of active and reactive powers under unbalanced voltage source is clearly demonstrated and the effect of grid fault on the performance of DFIG is profoundly discussed. Simulation results verified the effectiveness of the modified control strategy.*

Keywords: *DFIG,DPC-SVM, virtual flux, compensating power, grid fault*

NOMENCLATURE

1.1 Subscript
m:Mutual.
α, β: Two axis stationary reference frame.
d, q:Two-axis direct and quadrature synchronous reference frame.
s, r:Stator and rotor reference frame.
$+, -, 5$: Positive, negative sequence and harmonic component.

1.2 Superscript
θ, ω: Angle and angular speed.
τ, σ:Time constant and leakage factor.
e: Source voltage.
V: Converter terminals voltage.
i: Line current.
L, R: Input filter inductance and resistance.
P, Q: Apparent, active and reactive powers.
φ: Machine flux.
ψ : Virtual flux.

1.3 abbreviation
DFIG: Doubly fed induction Generator.
DPC : Direct power control
GSC: Grid side converter.
RSC: Rotor side converter.
PNSC:Positive-negative-sequence calculator.
PWM: Pulse width modulation.
SOGI: Second order general integrator.
SVM: Space vector modulation.

2. INTRODUCTION

Doubly fed induction generator (DFIG) connected to three level NPC back-to-back converter has been widely used in recent years due to its several advantages. Some of its advantages are speed operation, controllable power factor, improved system efficiency, very low harmonic distortion, low electromagnetic interferenceand most importantly, reduced converter rating, which is typically 30% of the generation rating , therefore, decreased cost and power loss [1-4].

One drawback of DFIG is its sensitivity to any grid distortion because the stator is directly connected to the grid. This fact may limit the use of DFIG especially in wind energy generation due to imposed electricity code. Hence the power injected in the grid must be performed [5-8].

The control of two level GSC under grid fault was firstly studied in the works of [9-12].Based on power analysis under grid unbalance, the referencing currents were calculated and then used in classical voltage oriented control. After that [13] generalized the study to GSC and RSC for DFIG. But the control became more complex when the grid is unbalanced and harmonically distorted.In addition, the tuning of PI gains constitutes a barrier to the use of this method.

In [13-16] a modified DPC for GSC and RSC was proposed to achieve one of three selective control targets: obtaining sinusoidal and symmetrical grid current, removing reactive power ripplesor removing active power ripples under unbalanced supply. The results obtained were good,but the study is in case of unbalance grid only. [17] Investigated the method of grid connected three level NPC converter and generalized the study to unbalanced and harmonically polluted grid. Thus, the introduction of voltage sensorless is a good alternative for robust and economic operation [18].

Virtual flux technique is the most responding technique for voltage sensorless control of GSC. In general, filters are used to estimate virtual flux [19-21]. But under unbalanced conditions, where the separating positive and negative sequences are needed, cascading filter must be used [22]. However, it creates more time delay and reduces the accuracy. Double second order generalized integrator (DSOGI) is a good alternative to remove the drawback of cascading filter, it could estimate the virtual flux and separate sequences of virtual flux and grid current [23].

This paper proposes a voltage sensorless control scheme for three level NPC back-to-back converter DFIG under unbalanced and harmonically polluted grid in order to get sinusoidal and symmetrical grid

and stator currents. To achieve that, the referencing current is calculated by the instantaneous power theory. The virtual flux isestimated using DSOGI method which is proposed by [23]. The effectiveness of the proposed method is verified by simulation in MATLAB environment.

The electrical circuit of the studied system is ullistrated in Figure1

3. MODELING OF DFIG

DFIG voltage and flux equations, expressed in the rotating reference frame, are given by:

$$\begin{cases} E_{sd} = R_s i_{sd} + \frac{d}{dt}\varphi_{sd} - \omega_s\varphi_{sq} \\ E_{sq} = R_s i_{sq} + \frac{d}{dt}\varphi_{sq} + \omega_s\varphi_{sd} \\ E_{rd} = R_r i_{rd} + \frac{d}{dt}\varphi_{rd} - \omega_r\varphi_{rq} \\ E_{rq} = R_r i_{rq} + \frac{d}{dt}\varphi_{rq} + \omega_r\varphi_{rd} \end{cases} \quad (1)$$

$$\begin{cases} \varphi_{sd} = L_s i_{sd} + L_m i_{rd} \\ \varphi_{sq} = L_s i_{sq} + L_m i_{rq} \\ \varphi_{rd} = L_r i_{rd} + L_m i_{sd} \\ \varphi_{rq} = L_r i_{rq} + L_m i_{sq} \end{cases} \quad (2)$$

Stator active and reactive powers are given by:

$$\begin{cases} P_s = E_{sd} i_{sd} + E_{sq} i_{sq} \\ Q_s = E_{sq} i_{sd} - E_{sd} i_{sq} \end{cases} \quad (3)$$

Setting the stator flux vector aligned to d-axis and neglicting the per phase stator resistance [15].

$$\begin{cases} \varphi_{sd} = \psi_s \\ \varphi_{sq} = 0 \end{cases} \quad (4)$$

$$\begin{cases} E_{sd} = 0 \\ E_{sq} = E_s = \omega_s\psi_s \end{cases} \quad (5)$$

Substuting in (2).

$$\begin{cases} \psi_s = L_s i_{sd} + L_m i_{rd} \\ 0 = L_s i_{sq} + L_m i_{rq} \end{cases} \quad (6)$$

The relation between the stator and rotor currents is set from equation(6):

$$\begin{cases} i_{sd} = -\frac{L_m}{L_s}i_{rd} + \frac{\psi_s}{L_s} \\ i_{sq} = -\frac{L_m}{L_s}i_{rq} \end{cases} \quad (7)$$
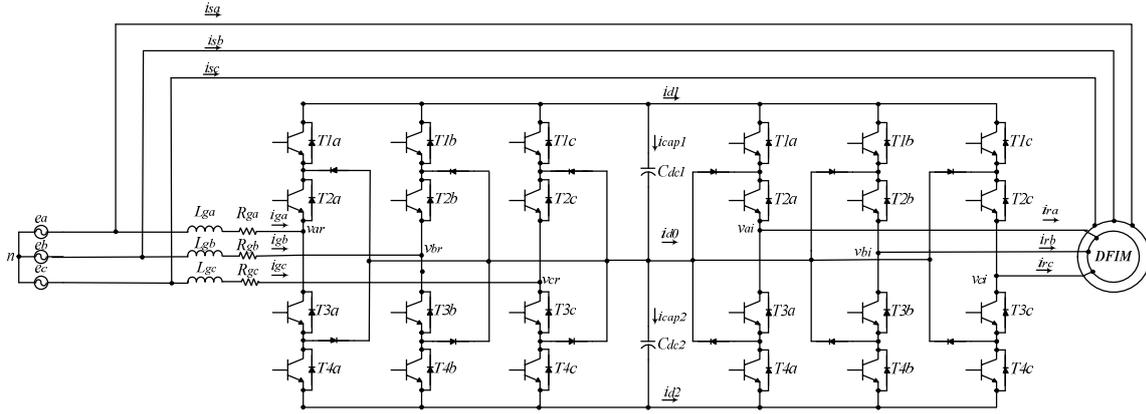
Figure.1. Simplified electrical circuit of a 3L-NPC back-to-back DFIG

Stator active and reactive powers in (3) can be written as:

$$\begin{cases} P_s = -E_s i_{sq} = -\frac{E_s L_m}{L_s} i_{rq} \\ Q_s = -E_s i_{sd} = -\frac{E_s L_m}{L_s} i_{rd} + \frac{E_s^2}{L_s \omega_s} \end{cases} \quad (8)$$

Rotor voltages can be expressed by:

$$\begin{cases} V_{dr} = R_r I_{rd} - g\omega_s \left(L_r - \frac{L_m^2}{L_s} \right) I_{rq} \\ V_{qr} = R_r I_{rq} + g\omega_s \left(L_r - \frac{L_m^2}{L_s} \right) I_{rd} + g \frac{L_m E_s}{L_s} \end{cases} \quad (9)$$

Figure.2 shows the detailed model of DFIG.
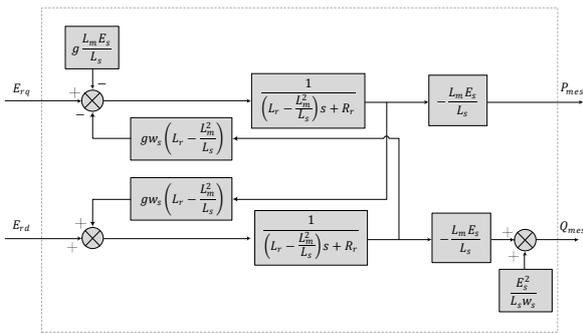
Figure.2. Simplified model of DFIG

4. CLASSICAL CONTROL STRATEGY

4.1. RSC control

If we neglect the coupling terms in equation (9), and replace (8) in (9) we can control the stator active and reactive powers. The measured statoricactive and reactive powers are compared with the referencing one, and then PI regulators are used as controllers. The output of PI regulators addedtocompensating terms provide the required rotor voltage as illustrated in Figure 3.
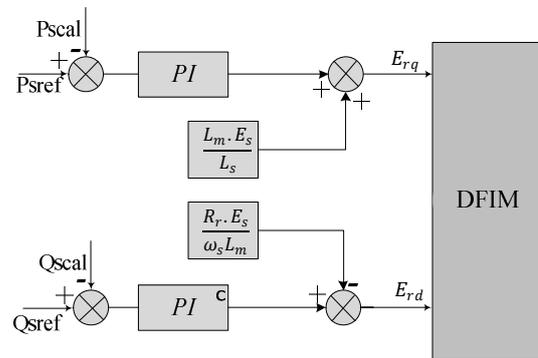
Figure.3. Direct active and reactive powerscontrol of DFIG

4.2. GSC control

For the GSC, the well known DPC-SVM is chosen as control algorithm which details is summarized in Figure 4. The outer control loop provide the required active power to obtain the desired dc-link voltage level.The measured active and reactive powers are compared with the referencing one, and then PI regulators are used as controllers instead look-up-table[24]. The two regulators provide the reference voltage applied to the input of the converter, after that the switching signals are generated by SVM block [25, 26].
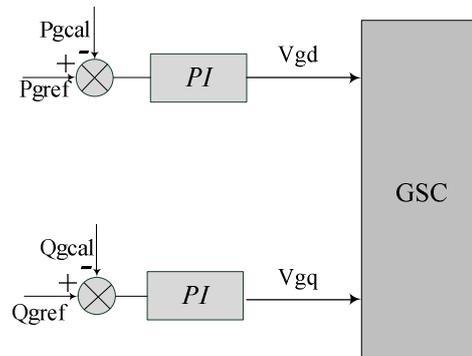
Figure.4. DPC-SVM control of GSC

5. POWER ANALYSIS UNDER GRID FAULT

5.1. Virtual flux estimation

Virtual flux (VF) concept is the most adopted method to estimate grid voltage for GSC.

By integrating ac-voltage we get the virtual flux as follows:

$$\psi_{g\alpha\beta} = \int E_{\alpha\beta} dt \qquad (10)$$

Replacing ac-voltage by its equivalent value extracted from the ac-side converter model we get:

$$\psi_{g\alpha\beta} = LI_{g\alpha\beta} + \int (Ri_{g\alpha\beta} + V_{g\alpha\beta}) dt \qquad (11)$$

$V_{g\alpha\beta}$ is estimated from the switching state and dc-link voltage.

Under ideal conditions, the VF has only positive-sequence components, but during grid fault, negative and harmonic sequences also appear in the virtual flux. And thus,positive,negative and harmonic sequences have to be separated in order to control the converter.Positive and negative sequence calculator (PNSC) is used to calculate the positive and negative sequences for each order harmonics.

As shown in Figure 5-a the PNSC needs the instantaneous values of the VF and its quadratic value. To get these values, Double Second Order Generalized Integrator (DSOGI) is one of the most feasible solutions proposed so far in the literature for its good results in terms of the accuracy and its capability for grid synchronization [23].

The transfer function for the SOGI-QSG is given by:

$$D(s) = \frac{U(s)}{U(s)} = \frac{k.\acute{\omega}s}{s^2 + k.\acute{\omega}.s + \omega^2} \qquad (12)$$

$$Q(s) = \frac{U(s)}{U(s)} = \frac{k.\omega'^2}{s^2 + k.\acute{\omega}.s + \omega'^2} \qquad (13)$$

The structure of (SOGI) is given in Fig.5-b. where the constant K is the SOGI gain that determines the system dynamics (k is selected as k $=\sqrt{2}$ for optimum value time response and overshoot).

The complete structure of virtual flux estimation with sequences separation is illustrated in Figure 6.

5.2. Powers equations

With the virtual flux approach active and reactive powers can be calculated from:

$$\begin{cases} P = \frac{3}{2}\omega(\psi_{g\alpha}I_{g\beta} - \psi_{g\beta}I_{g\alpha}) \\ Q = -\frac{3}{2}\omega(\psi_{g\alpha}I_{g\alpha} + \psi_{g\beta}I_{g\beta}) \end{cases} \qquad (14)$$

Using symmetrical component theory [27].

$$P_g = \frac{3}{2}\omega(\psi_{g\alpha}^+ I_{g\beta}^+ - \psi_{g\beta}^+ I_{g\alpha}^+ + \psi_{g\alpha}^- I_{g\beta}^- - \psi_{g\beta}^- I_{g\alpha}^- + \psi_{g\alpha}^5 I_{g\beta}^5 - \psi_{g\beta}^5 I_{g\alpha}^5 + \psi_{g\alpha}^+ I_{g\beta}^- - \psi_{g\beta}^+ I_{g\alpha}^- + \psi_{g\alpha}^- I_{g\beta}^+ - \psi_{g\beta}^- I_{g\alpha}^+ + \psi_{g\alpha}^+ I_{g\beta}^5 - \psi_{g\beta}^+ I_{g\alpha}^5 + \psi_{g\alpha}^5 I_{g\beta}^+ - \psi_{g\beta}^5 I_{g\alpha}^+ + \psi_{g\alpha}^5 I_{g\beta}^- - \psi_{g\beta}^5 I_{g\alpha}^- + \psi_{g\alpha}^- I_{g\beta}^5 - \psi_{g\beta}^- I_{g\alpha}^5) \qquad (15)$$

$$Q_g = -\frac{3}{2}\omega(\psi_{g\alpha}^+ I_{g\alpha}^+ + \psi_{g\beta}^+ I_{g\beta}^+ + \psi_{g\alpha}^- I_{g\alpha}^- + \psi_{g\beta}^- I_{g\beta}^- + \psi_{g\alpha}^5 I_{g\alpha}^5 + \psi_{g\beta}^5 I_{g\beta}^5 + \psi_{g\alpha}^+ I_{g\alpha}^- + \psi_{g\beta}^+ I_{g\beta}^- + \psi_{g\alpha}^- I_{g\alpha}^+ + \psi_{g\beta}^- I_{g\beta}^+ + \psi_{g\alpha}^+ I_{g\alpha}^5 + \psi_{g\beta}^+ I_{g\beta}^5 + \psi_{g\alpha}^5 I_{g\alpha}^+ + \psi_{g\beta}^5 I_{g\beta}^+ + \psi_{g\alpha}^5 I_{g\alpha}^- + \psi_{g\beta}^5 I_{g\beta}^- + \psi_{g\alpha}^- I_{g\alpha}^5 + \psi_g^- I_{g\beta}^5) \qquad (16)$$

Compared with active and reactive powers obtained under ideal voltages supply, many additional terms appear under grid fault. These terms result from the interaction between each sequence of the voltage (positive, negative and 5th harmonic) with the sequences of the current separately. These additional terms are responsible of the poor performance of the DFIG, especially the distorted stator currents.

According to equations (15) and (16) active and reactive powers can be regrouped in four terms:

$$P = \bar{P}_1 + \tilde{P}_2 + \tilde{P}_3 + \tilde{P}_4 \qquad (17)$$

Where:

$$\begin{cases} \bar{P}_1 = \frac{3}{2}\omega(\psi_{g\alpha}^+ I_{g\beta}^+ - \psi_{g\beta}^+ I_{g\alpha}^+ + \psi_{g\alpha}^- I_{g\beta}^- - \psi_{g\beta}^- I_{g\alpha}^-) \\ \qquad + \psi_{g\alpha}^5 I_{g\beta}^5 - \psi_{g\beta}^5 I_{g\alpha}^5 \\ \tilde{P}_2 = \frac{3}{2}\omega(\psi_{g\alpha}^+ I_{g\beta}^- - \psi_{g\beta}^+ I_{g\alpha}^- + \psi_{g\alpha}^- I_{g\beta}^+ - \psi_{g\beta}^- I_{g\alpha}^+) \\ \tilde{P}_3 = \frac{3}{2}\omega(\psi_{g\alpha}^+ I_{g\beta}^5 - \psi_{g\beta}^+ I_{g\alpha}^5 + \psi_{g\alpha}^5 I_{g\beta}^+ - \psi_{g\beta}^5 I_{g\alpha}^+) \\ \tilde{P}_4 = \frac{3}{2}\omega(\psi_{g\alpha}^5 I_{g\beta}^- - \psi_{g\beta}^5 I_{g\alpha}^- + \psi_{g\alpha}^- I_{g\beta}^5 - \psi_{g\beta}^- I_{g\alpha}^5) \end{cases}$$

$$(18)$$

P_1 is the average active power delivered to the stator and it is a constant power.

P_2 represents the interaction between the positive and the negative sequences of the voltages and the currents.

P_3 represents the interaction between the positive and the 5th harmonic sequences of the voltages and the currents.

P_4 represents the interaction between the negative and the 5th harmonic sequences of the voltages and the currents.

The same analysis was carried for the reactive power:
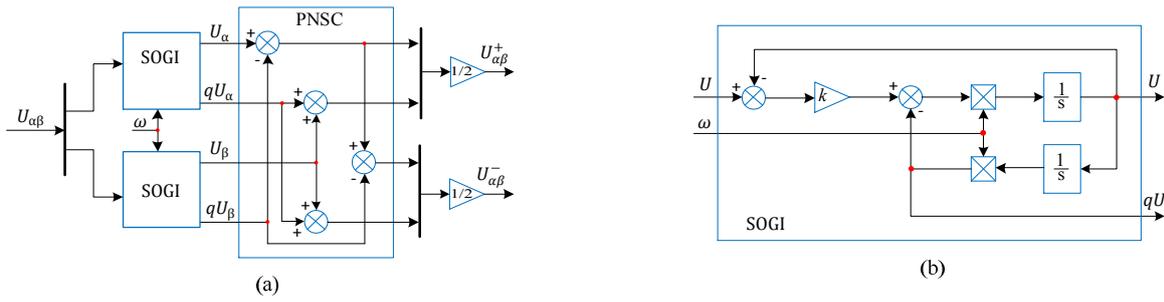
Figure.5. PNSC and SOGI structure
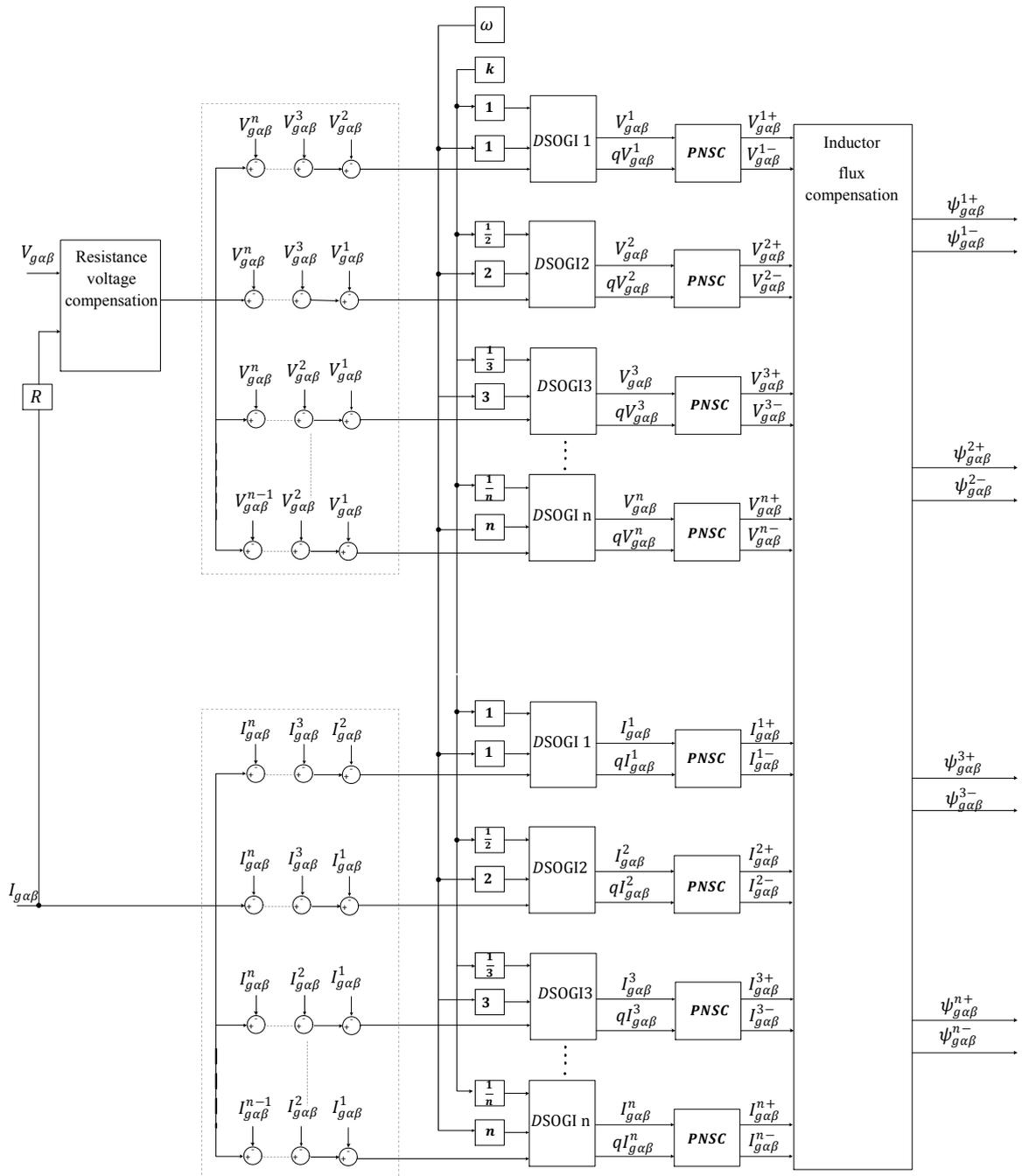
Figure.6. Complete structure of virtual flux estimation with sequence separation

$$Q = \bar{Q}_1 + \tilde{Q}_2 + \tilde{Q}_3 + \tilde{Q}_4 \qquad (19)$$

$$
\begin{cases}
\bar{Q}_1 = -\dfrac{3}{2}\omega(\psi_{g\alpha}^+ I_{g\alpha}^+ + \psi_{g\beta}^+ I_{g\beta}^+ + \psi_{g\alpha}^- I_{g\alpha}^- \\
\qquad\quad + \psi_{g\beta}^- I_{g\beta}^- + \psi_{g\alpha}^5 I_{g\alpha}^5 + \psi_{g\beta}^5 I_{g\beta}^5) \\
\tilde{Q}_2 = -\dfrac{3}{2}\omega(\psi_{g\alpha}^+ I_{g\alpha}^- + \psi_{g\beta}^+ I_{g\beta}^- + \psi_{g\alpha}^- I_{g\alpha}^+ + \psi_{g\beta}^- I_{g\beta}^+) \\
\tilde{Q}_3 = -\dfrac{3}{2}\omega(\psi_{g\alpha}^+ I_{g\alpha}^5 + \psi_{g\beta}^+ I_{g\beta}^5 + \psi_{g\alpha}^5 I_{g\alpha}^+ + \psi_{g\beta}^5 I_{g\beta}^+) \\
\tilde{Q}_4 = -\dfrac{3}{2}\omega(\psi_{g\alpha}^5 I_{g\alpha}^- + \psi_{g\beta}^5 I_{g\beta}^- + \psi_{g\alpha}^- I_{g\alpha}^5 + \psi_{g\beta}^- I_{g\beta}^5)
\end{cases}
$$

$$(20)$$

6. MODIFIED CONTROL STRATEGY

Classical DPC shows good performance under ideal voltage supply. But, unbalanced and or harmonically polluted grid voltages will result in significant low-order harmonic components in the grid and stator currents, which are caused by the negative and harmonic components in the voltages. Thus, in this paper, a modified strategy is proposed to improve the behavior of DFIG under grid fault.

For symmetrical and harmonic free components of stator/grid current we must make the negative component of current in equations (15) and (16) equal to zero so we get:

$$
\begin{cases}
P_g = \dfrac{3}{2}\omega(\psi_{g\alpha}^+ I_{g\beta}^+ - \psi_{g\beta}^+ I_{g\alpha}^+ + \psi_{g\alpha}^- I_{g\beta}^+ - \\
\qquad \psi_{g\beta}^- I_{g\alpha}^+ + \psi_{g\alpha}^5 I_{g\beta}^+ - \psi_{g\beta}^5 I_{g\alpha}^+) \\
Q_g = -\dfrac{3}{2}\omega(\psi_{g\alpha}^+ I_{g\alpha}^+ + \psi_{g\beta}^+ I_{g\beta}^+ + \psi_{g\alpha}^- I_{g\alpha}^+ + \\
\qquad \psi_{g\beta}^- I_{g\beta}^+ + \psi_{g\alpha}^5 I_{g\alpha}^+ + \psi_{g\beta}^5 I_{g\beta}^+)
\end{cases}
$$
$$(21)$$

omparing equations (21) and (14) we get the compensation power as:

$$
\begin{cases}
P_{gcomp} = \dfrac{3}{2}(\psi_{g\alpha}^- I_{g\beta}^+ - \psi_{g\beta}^- I_{g\alpha}^+ \\
\qquad\quad + \psi_{g\alpha}^5 I_{g\beta}^+ - \psi_{g\beta}^5 I_{g\alpha}^+) \\
Q_{gcomp} = \dfrac{3}{2}(\psi_{g\alpha}^- I_{g\alpha}^+ + \psi_{g\beta}^- I_{g\beta}^+ \\
\qquad\quad + \psi_{g\alpha}^5 I_{g\alpha}^+ + \psi_{g\beta}^5 I_{g\beta}^+)
\end{cases}
$$
$$(22)$$

The same analysis carried out for GSC was used to control RSC, substituting grid current by stator current in all active and reactive power equations.

7. SIMULATION RESULTS

Simulation studies of the GSC and RSC under unbalanced and grid fault conditions were carried out using MATLAB/simulink. The system parameters are given in the appendix.

The complete structure of the proposed control is shown in Figure7.

7.1 Balanced case

The grid is assumed balanced and perfectly sinusoidal with a change in the reference value of the active power of DFIG at instant 0.8 s (from -1.5 to -2MW) and an increase of the reactive power at instant 1s (from 0 to 30KVar) of GSC. The result are shown in Figs.8 to 12.

Figure.7. Control scheme under grid fault

Figure.8. Dc-link voltage, vdc1and vdc2
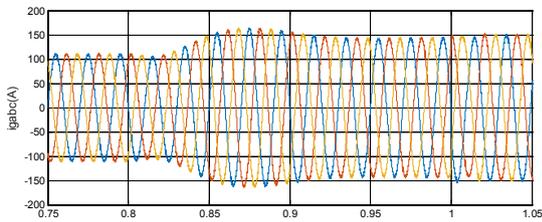
Figure.9. Grid current, voltage and current
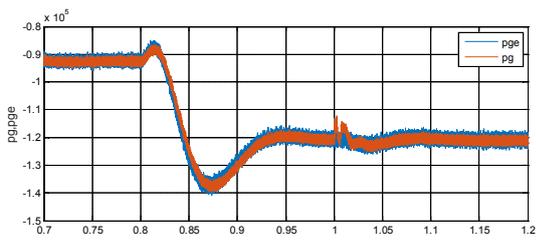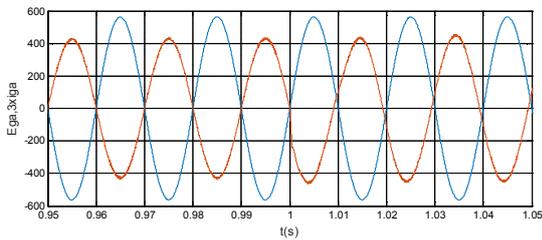
Figure.10. Grid estimated and measured active and reactive powers
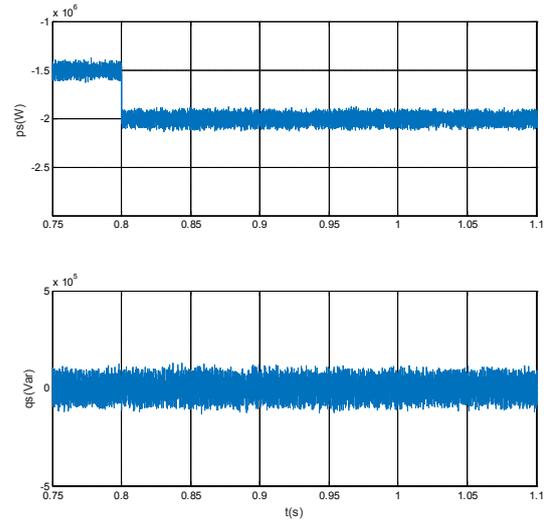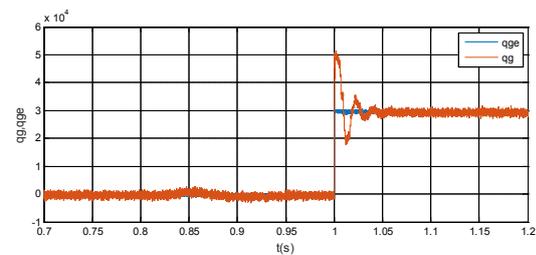
Figure.11. Stator active and reactive powers
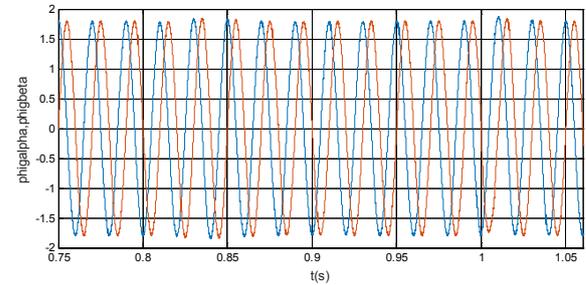
Figure.12. Virtual flux components

It is noted that DC voltage follows its reference and the balancing of continuous sources is always ensured as shown in Fig.8. Grid currents are sinusoidal and balanced with a unit power factor that shifts with the change in reactive power.

The change of the stator power causes a proportional variation in the power of GSC but does not affect the value of the continuous bus as well as the reactive power on the GSC.

The change of the reactive power on the grid causes a change in the power factor on the grid side, however, and all the other quantities remain practically unchanged.

The measured and estimated active and reactive powers are coincide as seen in Fig.10, so the DSOGI can estimate the active and reactive powers with infinite precision.

Figure12 shows the (α and β) component of the virtual flux. It is clear that the SOGI is able to estimate the virtual flow with a good dynamic and excellent robustness with respect to the changes made.

7.2 Unbalanced case

Introducing a voltage drop of 20% in phase 3 at time 0.7s then an overvoltage of 20% in phase 1 at time 0.8s. The compensation powers are injected at the instant 0.9s for GSC and 1s for RSC and the results obtained are shown in the figures above.
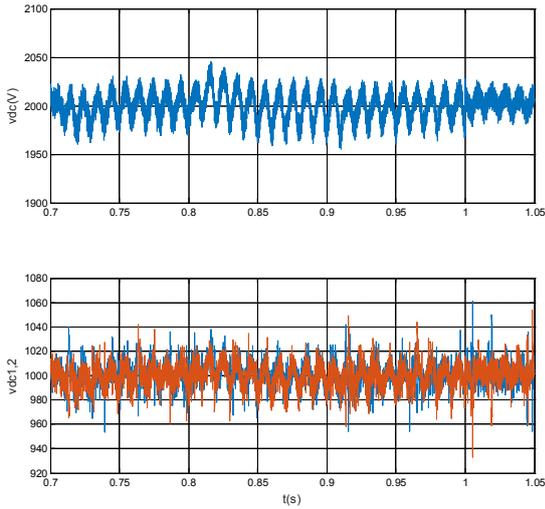
Figure.13. Dc-link voltage, vdc1and vdc2
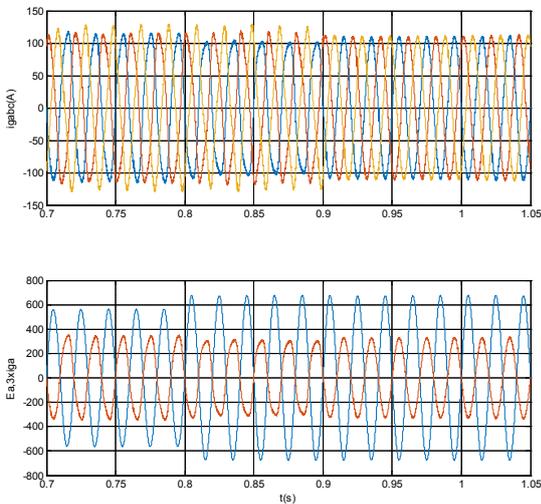
Figure.14. Grid current, voltage and current
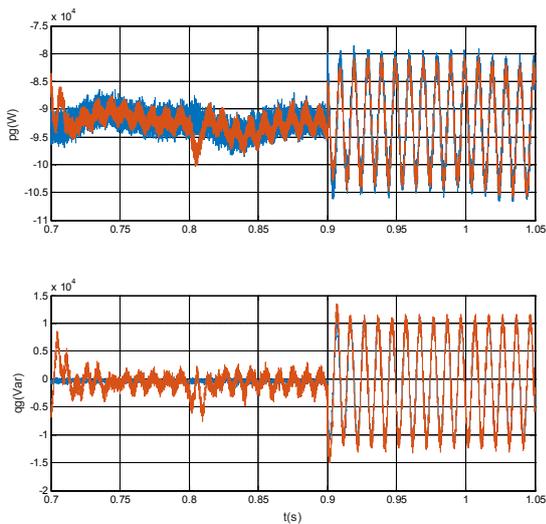
Figure.15. Grid estimated and measured active and reactive powers
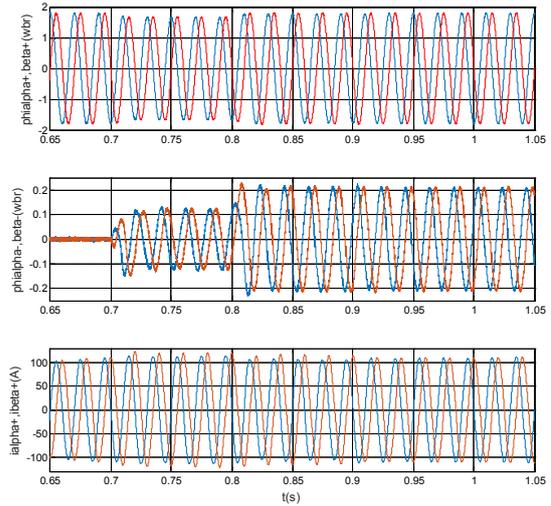
Figure.16. Positive, negative component of virtual flux and positive component of current

In Figures. 13~16, the behavior of the GSC has been demonstrated. After the introduction of the compensation powers, the system remained stable and the currents became balanced and sinusoidal with a unit power factor. The estimated and measured active and reactive powers are coincide with each other.

In Figure16, we see that the negative sequence of the virtual flux is zero before the instant 0.7s, then we detect a negative sequence with a transient time about 0.02s and its amplitude is amplified at instant 0.8s.
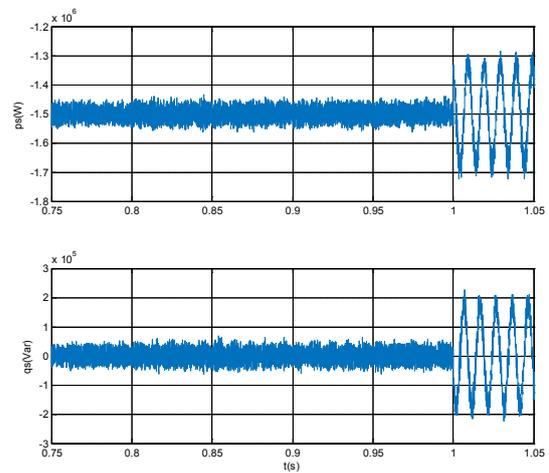
Figure.17. Stator active and reactive powers
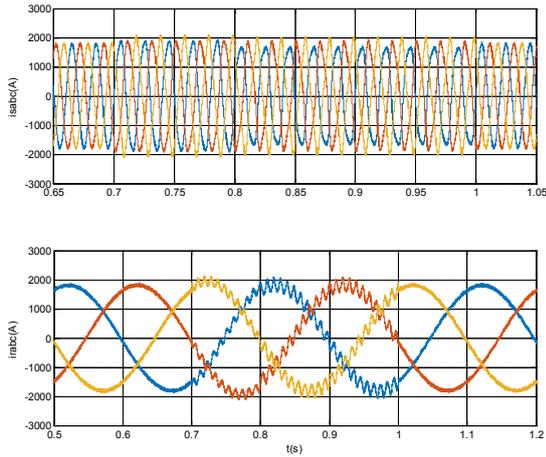
Figure.18. Stator and rotor current

Figure.19. Dc-link voltage, vdc1and vdc2

The same conclusion can be made for the GSC whose results are shown in Figures.17 and 18. It is observed that the control proposed is capable of improving the waveform of the stator currents by acting on the rotor variables. Stator currents become sinusoidal and balanced and rotor current fluctuations are minimized with the presence of ripples in the stator power.

7.3 Distorted case

To verify the wide validity of the proposed method, a test of the cascade under harmonically polluted grid was performed. In our case, the disturbance is the superposition of 20% of the 5th harmonic on the fundamental of the grid voltage. The system parameters and operating point are always kept the same as before.

The presence of the 5th harmonic in the grid creates pulsating terms in the DC voltage, their frequency is six times that of the grid frequency. The reflected pulses combined with the SVM fundamentals generate the 7^{th}order harmonic in the grid currents. These harmonics can be eliminated by applying the proposed command as shown in Figuress.19~22. The THD of the grid currents of the proposed control is only 1.19%, contrary to conventional methods which have a THD of 20.56%.

Figure.20. Grid current, voltage and current
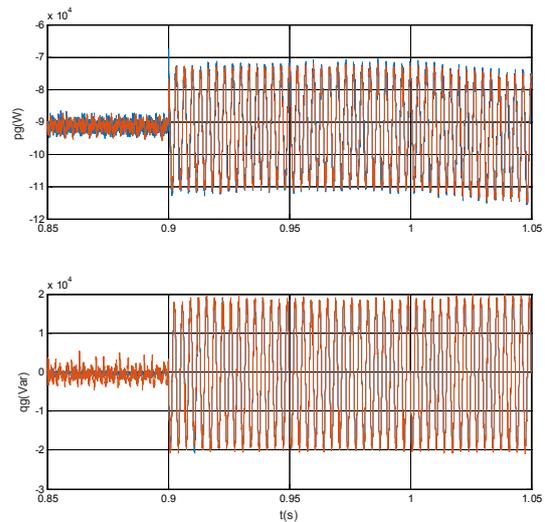
Figure.21. Grid estimated and measured active and reactive powers
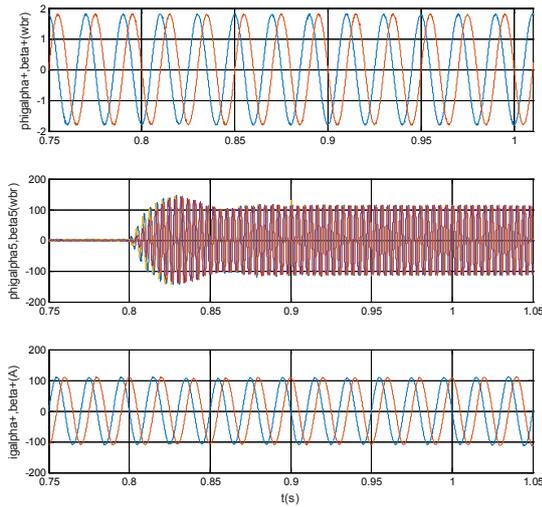
Figure ig.22. Positive, 5th harmonic component of virtual flux and positive component of current

Likewise, the grid fault has a harmful impact on the stator and rotor currents of the DFIG as shown in Figures.23 and 24. But after the injection of the compensation powers at the instant 1s, we observe a significant improvement in the waveform of the stator currents where the THD is decreased from 20.56 % to 3.94% driven by a minimization of the fluctuations in the rotor currents.
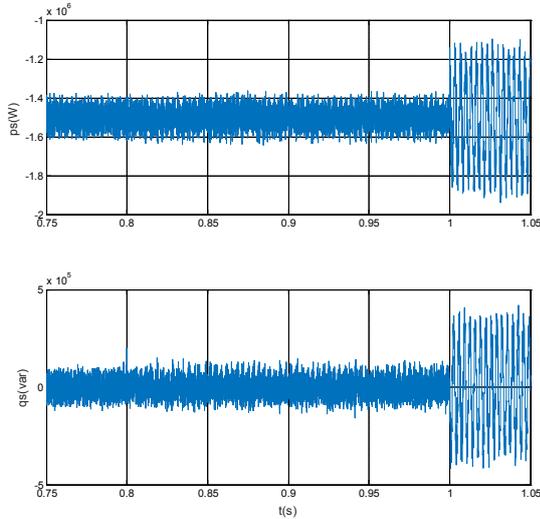
Figure.23. Stator active and reactive powers
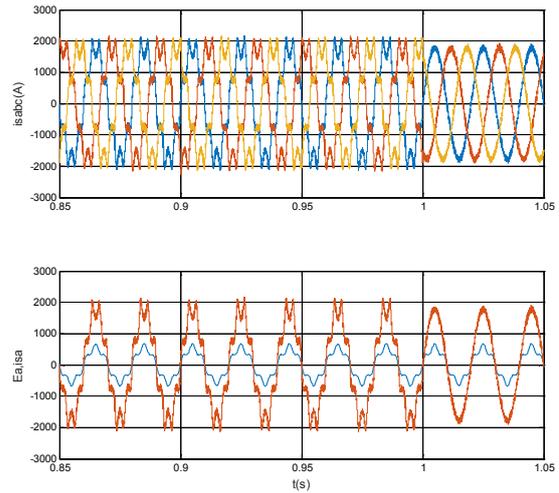
Figure.24. Grid current, voltage and current

7.4 Unbalanced and distorted case

Finally the system is tested under a very severe case where the imbalance and the harmonic are introduced together. As shown inFigures.25,26 and 27, the control technique proposed with the virtual flux always proves its validity under all conditions. The SOGI is capable of estimating and decomposing the virtual flux with precession and with good dynamics.

The target objective is achieved and, in our case, we were able to have sinusoidal and balanced currents on the grid and stator. The stability of the system is always assured in the different passages from the ideal to the abnormal.

Figure.25. From the top to the bottom: dc-link voltage, grid current, grid active and reactive powers

REFERENCES

1. Portillo, R. ; Vazquez, S.; Leon, J.I.; Parts, M.M and Franquelo, L.G." Model based adaptive direct power control for three-level NPC converters". IEEE Transactions on Industrial Informatics, vol. 9,no 2,pp. 1148–1157.2013.DOI: 10.1109/TII.2012.2209667.

2. BelkacemBelkacem, Abdelhakem-KoridakLahouari, RahliMostefa." Comparative Study between SPWM and SVPWM control of a three level voltage inverter dedicated to a variable speed wind turbine ". Journal of Power Technologies 97 (3) (2017) 190–200.

3. Alejandro, C.P; Salvador. A; Josep, B; Patricio, C.; and Jose, R "Predictive Control of a Back-to-Back NPC Converter-Based Wind Power System". IEEE Transactions on Industrial Electronics, vol 63,no7, pp.4615-4627,2016. DOI: 10.1109/TIE.2016.2529564.

4. Fangzhou Cheng and all, " Rotor-current-based fault diagnosis for DFIG wind turbine drivetrain gearboxes using frequency analysis and a deep classifier" IEEE Transactions on Industry Applications, vol.54 , no 2, pp. 1062 - 1071, 2018. DOI: 10.1109/TIA.2017.2773426.

5. David santos-martin, joseluis Rodriguez-amenedo and Santiago amalte" Direct power control Applied to doubly fed induction generator under unbalanced grid voltage conditions" IEEE Transactions on power electronics, vol.23, no.5. pp 2328-2335, 2008. DOI: 10.1109/TPEL.2008.2001907.

6. M. itsaso Martinez, Gerardo tapia, anasusperregui and haritzacamblong" DFIG power generation capability and feasibility regions under unbalanced grid voltage conditions" IEEE Transactions on energy conversion, vol.26, no. 4,pp.1051-1062, 2011. DOI: 10.1109/TEC.2011.2167976.

7. X. Y. Xiao, R. H. Yang, X. Y. Chen and Z. X. Zheng, "Integrated DFIG Protection With a Modified SMES-FCL Under Symmetrical and Asymmetrical Faults," in IEEE Transactions on Applied Superconductivity, vol. 28, no. 4, pp. 1-6, 2018. DOI: 10.1109/TASC.2018.2802782.

8. DehongXu,FredeBlaabjerg,Wenjie Chen ,Nan Zhu " Analysis of DFIG Under Distorted Grid Voltage" in . FredeBlaabjerg, DehongXu ,Wenjie Chen, Nan Zhu "Advanced Control of Doubly Fed Induction Generator for Wind Power Systems". 139 - 165Edition: 2018 1 Online ISBN: 9781119172093 Publisher: Wiley-IEEE Press. DOI: 10.1002/9781119172093.ch6

9. Eloy-Garcia, J.; Arnaltes, S ;andRedriguez-Amenedo, J.L." Direct power control of voltage source inverters with unbalanced grid voltages. IET Power Electron, vol. 1, no. 3,pp. 395– 407, 2007. DOI: 10.1109/TASC.2018.2802782.

10. Jiabing Hu, andYikang He, "Modeling and Control of Grid-Connected Voltage-Sourced Converters Under Generalized Unbalanced Operation Conditions", IEEE Transactions On Energy Conversion, vol. 23, no. 3, pp. 903-913, 2008. DOI: 10.1109/TEC.2008.921468.

11. Xiao, .P.; Corzine, K.A.; and Vena yagamoorthy, G.K" Multiple reference frame-based control of three-phase PWM boost rectifiers under unbalanced and distorted input conditions" IEEE Transactions on Power Electronics, vol.23, no.4, pp.2006–2017, 2008.DOI: 10.1109/TPEL.2008.925205.

Figure. 26. From the top to the bottom: Positive,negative, 5th harmonic component of virtual flux and positive component of current

Figure.27. Stator active and reactive powers, stator current, stator current and voltage

8. Conclusion

This paper has proposed sensorless compensated control scheme based on improved direct power control with space vector modulation (DPC-SVM) for doubly fed induction generator supplied by distorted grid voltage. In order to obtain sinusoidal grid and stator currents under grid distortion, compensated powers are calculated and added to the original referenced power to achieve balanced and high quality grid/stator current. The positive, negative and harmonic sequences of the virtual flux and the current are extracted using SOGI filter. The proposed method proves its capability of yielding sinusoidal grid and stator currentwith unity power factor under severe unbalanced voltage source.

12. Shang, L.; Sun, D.; and Hu, J. "Sliding-mode-based direct power control of grid connected voltage-sourced inverters under unbalanced network conditions" IET Power Electronics, vol. 4, no 5,pp. 570–579. 2011.DOI: 10.1049/iet-pel.2010.0160.

13. Jiabing Hu, hailiangXu and Yikang He " coordinated control of DFIG's RSC and GSC under generalized unbalanced and distorted voltage conditions" IEEE Transactions industrial electronics, vol. 60, no.7,pp. 2808-2019, 2013. DOI: 10.1109/TIE.2012.2217718.

14. Shang L, Hu J" Sliding-mode-based direct power control of grid-connected wind- turbine-driven doubly fed induction generators under unbalanced grid voltage conditions" IEEE Transactions on Energy Conversion, vol. 27,no.2, pp. 362–373,2012 . DOI: 10.1109/TEC.2011.2180389.

15. HengNian and Yipeng song "Direct power control of doubly fed induction generator under distorted grid voltage" IEEE Transactions on power electronics, vol. 29, no. 2, pp. 894-905, 2014. DOI: 10.1109/TPEL.2013.2258943

16. J.S. Solís-Chaves and all " A direct power control for DFIG under a three phase symmetrical voltage sag condition" Control Engineering Practice, vol 65,pp 48–58, 2017. https://doi.org/10.1016/j.conengprac.2017.05.002

17. Imad Merzouk, Mohamed LokmaneBendaas "Improved direct power control for 3-level AC/DC converter under unbalanced and/or distorted voltage source conditions" Turkish Journal of Electrical Engineering & Computer Sciences, vol. 24, no.3, pp. 1847-1862, 2016.

18. Haitao Yang, Yongchang Zhang, Nong Zhang, Paul D Walker and JihaoGao, "A voltage sensorless finite control set-model predictive control for three-phase voltage source PWMrectifiers". Chinese Journal of Electrical Engineering, vol. l0 ,no.3 , pp. 52 - 59, 2016. DOI: 10.23919/CJEE.2016.7933126.

19. Yong, S. C.; and Lee, K.B."Virtual-Flux-Based Predictive Direct Power Control of Three-Phase PWM Rectifiers with Fast Dynamic Response". IEEE Transactions On Power Electronics, vol. 31, no. 4,pp. 3348-3359,2016. DOI: 10.1109/TPEL.2015.2453129.

20. Xiong Xiao ; Yongjun Zhang ; Xian Song ; TanjuYildirim ; Fei Zhang "VirtualFluxDirectPowerControl for PWM Rectifiers Based on an Adaptive Sliding Mode Observer" IEEE Transactions on Industry Applications, Vol. 54 , no. 5, pp. 5196 - 5205, 2018. DOI: 10.1109/TIA.2018.2832122.

21. Zhenbin Zhang, He Xu, Ming Xue, Zhe Chen, Tongjing Sun, Ralph Kennel, and Christoph M. Hackl, "Predictive Control With Novel Virtual-Flux Estimation for Back-to-Back Power Converters". IEEE Transactions On Industrial Electronics, vol. 62, no. 5, pp. 2823-2834,2015. DOI: 10.1109/TIE.2014.2361802.

22. Pedro Rodríguez, Alvaro Luna, Ignacio Candela, Ramon Mujal, Remus Teodorescu, and FredeBlaabjerg, "Multiresonant Frequency-locked Loop for Grid Synchronization of Power Converters Under Distorted Grid Conditions". IEEE Transactions On Industrial Electronics, vol. 58, no. 1, pp.127-138, 2011. DOI: 10.1109/TIE.2010.2042420.

23. Jon Are Suul; Alvaro Luna; Pedro Rodríguez; Tore Undeland, "Virtual-Flux-Based Voltage-Sensor-Less Power Control for Unbalanced Grid Conditions". IEEE Transactions on Power Electronics, vol. 27, n, pp. 4071 - 4087, 2012.DOI: 10.1109/TPEL.2012.2190301.

24. Yong, chang, Z.; and Chang, Qu." Table-Based Direct Power Control for Three-Phase AC/DC Converters under Unbalanced Grid Voltages". IEEE Transactions On Power Electronics, vol. 30, no12, pp. 7090-7099,2015.DOI: 10.1109/TPEL.2014.2387694.

25. Kulikowski, K.; and Sikorski, A." New DPC Look-Up Tabl e Methods for Three-Level AC/DC Converter". IEEE Transactions On Industrial Electronics, vol.63,no12,pp. 7930-7938. 2016. DOI: 10.1109/TIE.2016.2538208.

26. Dan, S. ; Xiao, H.W. ; Yang, F. Backstepping "Backstepping direct power control without phase-locked loop of AC/DC converter under both balanced and unbalanced grid conditions "IET Power Electronics, vol.9,no 8,pp. 1614–1624, 2016. DOI: 10.1049/iet-pel.2015.0653.

27. Yashan Hu, ZiQiang Zhu, *IEEE*, and MilijanaOdavic" Instantaneous Power Control for Suppressing the Second-Harmonic DC-Bus Voltage Under Generic Unbalanced Operating Conditions" IEEE Transactions On Power Electronics, vol. 32, no. 5, 2017. DOI: 10.1109/TPEL.2016.2584385.

Appendix

Table 1. Power circuit parameters

Items	Symbol	Value
Nominal Power	P	2MW
Stator resistance	R_s	12 $m\Omega$
Rotor resistance	R_r	21 $m\Omega$
Stator inductance	L_s	0.0137 H
Rotor inductance	L_r	0.01367 H
Mutual inductance	L_m	0.0135H
Number of pole pairs	P	2
Input filter inductance	L	12mH
Input filter resistance	R	0.3Ω
Dc-bus capacitor	C_{dc}	500μF
DC voltage	V_{dc}	400V
AC source voltage	e	690V